Published in final edited form as:
J Pharm Sci. 2010 July ; 99(7): 3072–3080. doi:10.1002/jps.22083.

Transdermal delivery of naltrexol and skin permeability lifetime after microneedle treatment in hairless guinea pigs

Stan L. Banks[a], **Raghotham R. Pinninti**[a], **Harvinder S. Gill**[b], **Kalpana S. Paudel**[a], **Peter A. Crooks**[a], **Nicole K. Brogden**[a], **Mark R. Prausnitz**[b,c], and **Audra L. Stinchcomb**[a]

[a]Department of Pharmaceutical Sciences, University of Kentucky College of Pharmacy, Lexington, Kentucky 40536-0082

[b]The Wallance Coulter School of Biomedical Engineering at Georgia Tech and Emory University, Georgia Institute of Technology, Atlanta, GA 30332-0363

[c]School of Chemical and Biomolecular Engineering, Georgia Institute of Technology, Atlanta, GA 30332-0100

Abstract

Controlled-release delivery of 6-β-naltrexol (NTXOL), the major active metabolite of naltrexone, via a transdermal patch is desirable for treatment of alcoholism. Unfortunately, NTXOL does not diffuse across skin at a therapeutic rate. Therefore, the focus of this study was to evaluate microneedle (MN) skin permeation enhancement of NTXOL's hydrochloride salt in hairless guinea pigs. Specifically, these studies were designed to determine the lifetime of MN-created aqueous pore pathways. Microneedle pore lifetime was estimated by pharmacokinetic evaluation, transepidermal water loss (TEWL) and visualization of MN-treated skin pore diameters using light microscopy. A 3.6 fold enhancement in steady state plasma concentration was observed *in vivo* with MN treated skin with NTXOL·HCl, as compared to NTXOL base. TEWL measurements and microscopic evaluation of stained MN-treated guinea pig skin indicated the presence of pores, suggesting a feasible non-lipid bilayer pathway for enhanced transdermal delivery. Overall, MN-assisted transdermal delivery appears viable for at least 48 h after MN-application.

Keywords

Microneedle; 6-β-naltrexol; transdermal; hairless guinea pig; addiction therapy

Introduction

The treatment of opiate and alcohol addiction is of great societal importance today. In 2001 the World Health Organization reported that of the leading causes of disability worldwide, alcohol abuse is ranked in the top ten.[1] The annual economic cost of alcohol abuse and its related problems has been estimated at well over $100 billion and an additional $100 billion has been spent on problems occurring from other drugs of abuse.[2] Between 1991 and 2001, spending on mental health and drug abuse grew from $60 billion to $104 billion.[3] Current available therapies for addicts include methadone and buprenorphine for opiate addicts, acamprosate for alcoholics, and ReVia® (50 mg oral dose of naltrexone HCl) for opiate and alcohol addicts. Vivitrol® was approved by the FDA in 2006 for the treatment of alcoholism.[4,5] Vivitrol is marketed as a 380 mg naltrexone depot formulation that is implanted underneath

*Corresponding author: Audra L. Stinchcomb (astin2@email.uky.edu), Tel.: 859-323-6192, Fax: 859-257-2787.

the skin every 28 d.[4] The oral form, ReVia®, is poorly bioavailable and has many documented side effects.[5] Patients undergoing Vivitrol therapy would not be able to be easily treated with opiates for emergency pain unless very high and potentially toxic doses of opiate drugs were used. Adverse reactions and negative side effects to these undesirable dosage forms of naltrexone could result in discontinuation of therapy and ultimately relapse into a using state.

6-β-Naltrexol (NTXOL), the major active metabolite of naltrexone (NTX), has long been thought to be a clinically useful molecule for alcohol abuse treatment. Both NTX and NTXOL solutions were able to reduce the consumption of ethanol in rats, suggesting a possible role for NTXOL therapy alone.[6,7] Also, studies have shown that NTXOL has an increased terminal half-life and a higher plasma concentration in humans after oral dosing, as compared to NTX.[8-11] Higher plasma drug concentrations that may be more effective, as well as a longer duration of action would make NTXOL an excellent alternative therapy to NTX.

Microneedle (MN) treatment of skin to bypass the stratum corneum, the major barrier to transdermal delivery, is a novel physical permeation enhancement method.[12] Composed from silicon, glass, stainless steel and biodegradable polymers, microneedles are manufactured by adapting microfabrication technology developed by the microelectronics industry.[13,14] In vitro and animal studies have established the ability of microneedles to deliver a variety of compounds across the skin, including insulin, desmopressin, oligonucleotides, DNA and a variety of vaccines.[15-19] Recent clinical studies have addressed delivery to humans of naltrexone[20], parathyroid hormone[21] and influenza vaccine[22]. A variety of microneedle designs were also shown to cause little or no pain in comparison to a 26-gauge hypodermic needle.[23] Thus, microneedles may provide an alternative pathway to enhance the permeation of large and poorly lipid-soluble compounds.

This study sought to evaluate the effect of microneedle pretreatment of the skin on the delivery of NTXOL·HCl and NTXOL free base from topical 2% hydroxyethylcellulose gel formulations. We hypothesized that microneedle pretreatment increases transdermal delivery of both of the compounds and that microneedles increase NTXOL·HCl deliver to a greater extent than NTXOL free base. The focus of the present study was to determine the lifetime *in vivo* of the aqueous channels created by MN treatment in the hairless guinea pig pharmacokinetic model. We further hypothesized that pores created by microneedles can remain open for 48 hours.[20] Besides measurement of skin permeability to NTXOL to determine pore lifetime, transepidermal water loss (TEWL) measurements were utilized after MN treatment along with microscopic visualization. TEWL values are commonly measured in compromised skin to determine water loss over time as a function of skin repair.[24] In addition, a staining technique was developed to evaluate MN-treated guinea pig skin to microscopically visualize microneedle created pores. Finally, in order to determine skin irritation resulting from topical treatments *in vivo*, erythema was monitored with a colorimeter.

Materials and Methods

Chemicals and films

NTX base was purchased from Mallinckrodt (St. Louis, MO). 1,2-propanediol (propylene glycol) was purchased from Sigma-Aldrich (St. Louis, MO). Natrosol® (hydroxyethylcellulose) was a gift from Hercules Inc. (Wilmington, DE). Ammonium acetate, ammonium citrate, ethyl acetate, methylparaben, propylparaben and acetonitrile (ACN) were obtained through Fisher Scientific (Fairlawn, NJ). Occlusive backing membrane, Scotchpak™ #1109 SPAK 1.34 MIL Heat Sealable Polyester Film, was a gift from 3M™ (St. Paul, MN). ARcare® 7396 (pressure-sensitive tape with MA-38 medical grade acrylic adhesive) was a gift from Adhesives Research, Inc. (Glen Rock, PA). Scotchpak™ 9742, a fluoropolymer release liner, was a gift from 3M™ Drug Delivery Systems (St. Paul, MN). Water was purified by a

Barnstead NANOpure® Diamond™ Ultrapure water system (Barnstead International, Dubuque, IA).

Microneedle fabrication

Microneedle arrays were prepared as described below and methods previously described by Martanto *et al.* [17] In-plane microneedle rows with five microneedles each were cut from stainless steel sheets (Trinity Brand Industries, SS 304, 75 mm thick; McMaster-Carr, Atlanta, GA) using an infrared laser (Resonetics Maestro, Nashua, NH). Briefly, the microneedle row was first drafted in AutoCAD® software (Autodesk®, San Rafael, CA). Using this design, the infrared laser was used to cut microneedles into the stainless steel sheet. The microneedle rows while still in place in the stainless steel sheets, were then cleaned with detergent (Alconox, White Plains, NY) to de-grease the surface and remove part of the slag and oxides deposited during laser-cutting. To completely clean the debris and to sharpen microneedle tips, microneedle rows were electropolished in a solution containing glycerin, ortho-phosphoric acid (85%) and water in a ratio of 6:3:1 by volume (all chemicals, Fisher Scientific). Electropolishing was performed in a 300 mL glass beaker at 70°C, a stirring rate of 150 rpm, with a current density of 1.8 mA/mm^2 applied for 15 min. A copper plate was used as the cathode, while microneedles acted as the anode. The electropolished microneedle rows were then cleaned by alternatively dipping in 25% nitric acid (Fisher Scientific) and deionized water with a total of three repetitions. A final rinse was performed under running deionized water before drying under pressurized air. Dry microneedle rows were stored in air-tight containers. Each microneedle measured 750 μm in length, had a base width of 180 μm, and <1 μm radius in curvature at the tip. The distance between individual MN's is approximately 1 mm. Figure 1 depicts the microneedle rows and assembled microneedle array containing a total of 50 MN's.

6-β-Naltrexol base

Synthesis procedures were performed with minor modifications as described by Paudel *et al.* 25،26 One-hundred mL of 0.533 M aqueous NaOH was added to NTX free base (13.6 g, 40.0 mmol) in an aqueous suspension under argon.26 The alkaline solution of NTX was treated dropwise at ambient temperature for 20 min with 17.4 g (80 mmol) of formamidine sulfinic acid dissolved in 200 mL of 0.533 M aqueous NaOH. After the addition was complete, the solution was heated and stirred at 80-85°C for 1.5 h when thin layer chromatography analysis indicated the reaction to be complete.26 The reaction mixture was cooled (ice bath) and then treated drop wise under argon with a solution of ammonium chloride (10.27 g, 192 mmol) in distilled water (100 mL). The aqueous mixture was extracted with 5 × 100 mL of $CHC1_3$, and the combined organic extract was filtered through a pad of Na_2SO_4 and evaporated *in vacuo* to afford the crude product (free base) as a foam, which was dissolved in 20 mL of warm (50° C) ethyl acetate and diluted to 60 mL with warm n-hexane.[26] Crystallization occurred spontaneously on cooling. The crystals were collected by filtration, washed with 2 × 10 mL of cold ethyl acetate/n-hexane (1:3) and oven-dried *in vacuo* at 60°C to give NTXOL: ′H NMR ($CDC1_3$) 6.71 (d, J = 8.1 Hz, 1 H), 6.56 (d, J = 8.1 Hz, 1 H), 4.55 (d, J = 6.1 Hz, 1 H), 3.57 (m, 1 H), (MP 185°C).

Gel formulations

21.7 % w/w NTXOL·HCl gels were prepared for *in vivo* studies. Hydrochloride salt gels were formulated by dissolving 21.5 % NTXOL·HCl, 0.15 % propylparaben, 0.05% methylparaben and 2.0 % hydroxyethylcellulose polymer in 76.1% 3:1 propylene glycol: H_2O (PG:H_2O). As the polymer was dissolved, the solution was vortexed and sonicated to ensure solvation as well as to initiate polymerization. The solution was sonicated for 20 min, briefly removing to vortex periodically. A viscous gel resulted, transparent in nature, and no visible solid particles were observed. A 2.5 % w/w naltrexol base gel was also prepared as described above adjusting only

the solvent percentage to obtain 100% mass balance. The NTXOL base gel was saturated with excess solid and therefore was a cloudy gel. Placebo gels were also prepared, consisting of the aforementioned excipients, at 0.15 % propylparaben, 0.05 % methylparaben and 2.0 % hydroxyethylcellulose polymer in 3:1 PG:H_2O.

Fabrication of transdermal patches of NTXOL and gel formulation

Transdermal patches—The transdermal occlusive protective covering patches of NTXOL base or HCl (6.7 cm^2) were fabricated by sandwiching a rubber ringed barrier to create a reservoir between a drug-impermeable backing membrane (Scotchpak™ #1109 SPAK 1.34 MIL Heat Sealable Polyester Film) and an ARcare® 7396 adhesive around the edge of the rubber spacer. The impermeable backing laminate was adhered to the rubber retaining ringed barrier with 3M™ double sided tape. Finally, ARcare® 7396 was placed on the bottom of the rubber ringed barrier to maintain intimate contact with the skin and prevent evaporation of the 500 μL gel formulations. The protective patch was placed on a release liner composed of Scotchpak™ 9742 until applied to a guinea pig.

In vivo studies

Microneedle Insertion: For all studies, microneedle array application was performed by one individual to decrease variability in pressure applied during application. In an earlier work by Davis, S.P. et al., the force determined to provide ample insertion was approximately 1.0 – 3.0 N, or the pressure applied when pressing an elevator button.[27] Martanto et al. showed using a similar needle that full insertion was observed in the skin[17], and coupled with an adhesive layer surrounding the MN array, full insertion upon application should be achieved. Gill et al. also showed greater than 90% insertion with a coated MN of similar composition and just less than 100% of coated material was deposited in the skin.[28] After insertion the array was removed and either an occlusive patch or a gel followed by an occlusive patch was immediately placed over the treated area. Occasionally, extracellular fluid could be observed after MN insertion, however at the end of each study the skin showed little or no evidence of disruption.

Transepidermal water loss *in vivo*—In order to measure the rate of pore resealing after MN treatment, transepidermal water loss (TEWL, cyberDERM, Media, PA) was employed.[24] Control areas of skin were covered with an empty occlusive patch and treated areas on the GP were subjected to 100 MN insertions plus an empty occlusive patch. Both areas were measured with the TEWL evaporimeter that estimates water loss, which is derived from the difference in the vapor pressures of the skin and an area 4 mm above the skin.24 TEWL measurements were made over time until measurements return to a baseline level that corresponds to TEWL measurements of untreated skin with no occlusive covering. Measurements were obtained in less than 30 s and the skin areas were immediately re-covered with adhesive patch dressing. The evaporimeter measured water loss from hairless guinea pigs in units of $g/m^2/h$.

Skin irritation of MN and gel treated areas *in vivo*: Hairless guinea pigs were treated with MN arrays and had either NTXOL base or HCl gel applied to the skin. A placebo gel was also applied to an animal with MN treatment on one side and intact skin on the other. After 72 h, patches and gel were removed and measurements for skin erythema were made with a colorimeter 29 (Chroma Meter CR-400, Konica Minolta, Japan) over a 48 h post gel removal interval. The color reflectance was recorded in three-dimensional scale L*a*b.[30] The L* value (luminance) expressed the relative brightness of the color ranging from total black (L* = 0) to pure white (L* = 100). The a* reading was the red-green axis with +100 expressing full red and -100 full green, and b* was the yellow-blue axis. Previous studies show that skin irritation should have decreased the L* value and increased the a* value. The colorimeter was calibrated each day against a white plate provided by Konica Minolta in the study environment. For

measurement, the head of the instrument was gently placed on the skin area where the patch was applied.

Microscopic visualization of MN channels *in vivo*: Hairless guinea pigs were treated with microneedle arrays at time 0, 24 h, 48 h and 72 h and had an occlusive patch placed over the treatment site at each time point. The occlusive patch was prepared as described by Paudel *et al.*[28] except that no drug solution was placed in each patch. Each treated animal was sacrificed and treated skin areas were removed for microscopic visualization. The final MN application at 72 h was made 10 minutes prior to the animal being sacrificed. Pore lifetime visualization after MN application was thus observed as a control area (no MN), 10 minute, 24, 48, and 72 h time periods after MN application. Each skin sample was coated with India ink, washed with methanol and water, and then mounted on a microscope slide for analysis. Skin samples were visually analyzed with an Olympus® SZX12 stereoscope. Images were acquired with a QColor3™ camera by Olympus® America Inc. (Center Valley, PA), and analyzed with QCapture Pro 5.1 (Q Imaging®) (Surrey, BC, Canada).

Pharmacokinetic animal studies: Male and female hairless IAF guinea pigs (Charles River) weighing 350–650 g were used for these studies. All animal studies were in accordance with the institutional guidelines and approved by the University of Kentucky IACUC. Surgical procedure was performed to canulate the jugular vein. Blood samples (0.3 mL) were drawn from the jugular vein at regular time intervals for the time studied. MN treated animals were first cleaned topically with isopropyl alcohol, and two 50 MN arrays were then manually applied to each dose site. For topical delivery studies with or without MN treated GPs, two 0.5 mL gel doses were applied to the dorsal region of the hairless guinea pigs. Blood samples were obtained for 72 h while the patch was on the animal and another 24 h after patch removal. The blood samples were immediately centrifuged at 10,000 × g for 3 min; plasma was separated and stored at −70°C until analysis.

Analytical method of NTXOL in plasma samples

Analytical method of NTXOL in plasma samples: ***Plasma sample extraction procedure:*** Samples were prepared and analyzed as described by Paudel *et al.*[25] One-hundred μL of plasma was extracted with 500 μL of ACN: ethyl acetate (1:1 v/v). The mixture was vortexed for 30 s and centrifuged at 10,000 × g for 12 min. The supernatant was pipetted into a 3 mL glass test tube and evaporated under nitrogen at 37°C. The residue was reconstituted with 100 μL of ACN and sonicated for 15 min. The samples were transferred into autosampler vials containing low volume inserts, and 20 μL was injected onto the HPLC column. The extraction efficiency was 92 ± 5% for NTXOL.

Liquid chromatography: Chromatography was performed on a Waters Symmetry® $C1_8$ (2.1 × 150mm, 5 μm) column at 35°C with a mobile phase consisting of ammonium acetate (2 mM) containing 0.01 mM of ammonium citrate:ACN (65:35 v/v) at a flow-rate of 0.25 mL/min.

Mass spectrometry: The system consisted of an HPLC with mass spectrometry detection (LC-MS) equipped with a Waters Alliance 2695 pump, Alliance 2695 autosampler, and a Micromass ZQ detector (Milford, MA) using electrospray ionization (ESI) for ion production. Selected ion monitoring (SIM) was performed in positive mode for NTXOL, m/z 344 $[M+H]^+$. Capillary voltage was 4.5 kV and cone voltage was 30 V. The source block and desolvation temperatures were 120°C and 250°C, respectively. Nitrogen was used as a nebulization and drying gas at flow rates of 50 and 450 L/h, respectively. The retention time of NTXOL was 4.81 ± 0.15 min. Intraday specificity for 10 and 25 ng/mL was 6.4 % Relative Standard Deviation (RSD) and 9.7 %RSD, respectively.

In vivo data analysis: The pharmacokinetic analysis of NTXOL plasma concentration versus time profiles after MN treatment and gel patch application was carried out by fitting the data to a noncompartmental model with extravascular input (WinNonlin Professional, version 4.0, Pharsight Corporation, Mountain View, CA). The data generated after transdermal application were analyzed by a noncompartmental method using WinNonlin® to determine peak concentration (C_{max}), steady state concentration (C_{ss}), lag time to steady state concentration (t_{lag}), and area under the plasma concentration time course from 0 to 48 h (AUC_{0-48}). The steady state plasma concentration of NTXOL after the application of patches was calculated by using the equation $C_{ss}= AUC_{0-t}/time$.

Statistical analysis of the *in vivo* data obtained after the transdermal application of the patches was performed by one-way ANOVA using SigmaStat.

Results and Discussion

Pharmacokinetic evaluation of in vivo studies

Following the described procedures, permeation of NTXOL base and HCl salt were studied in hairless guinea pigs, either treated with MN arrays or simply by passive diffusion. Following microneedle array (Fig. 1) treatment, the gel patch system was applied for 72 h to confirm previously discussed findings that MN-created pores are viable within the 48–72 h window determined by TEWL and microscopic evaluation of MN-pores. A summary of the pharmacokinetic parameters is shown in Table 1. As expected, the plasma profiles in Fig. 2 show low levels of NTXOL from NTXOL base (□) and NTXOL·HCl (Δ) when the skin is not first subjected to MN treatment. The steady state concentrations from base and HCl salt were 1.0 ± 0.4 and 1.0 ± 0.7 ng/mL, respectively (Table 1). Similar results were obtained for NTXOL base by Paudel *et al*, where a steady state concentration of 3.64 ± 0.45 ng/mL was found *in vivo*[25]. MN treated animals with NTXOL base did show enhancement in the hairless guinea pig model, but only to a steady state concentration of 5.5 ± 1.9 ng/mL. Compared to highly water soluble NTXOL·HCl, which had a determined steady state concentration of 21.3 ± 6.19 ng/mL, NTXOL base MN enhancement was four-fold less ($p<0.05$). This trend is clearly evident in Fig. 2 showing significant enhancement of MN treated hairless GP's with NTXOL·HCl (▲) and NTXOL base (■). High permeation of a water soluble salt is percutaneously impractical, but with MN application, the permeation barrier is bypassed and desired levels of a poorly permeable compound can be achieved. As for the higher permeation of NTXOL base through MN treated skin, two factors can explain the driving force for the limited enhanced permeation of the lipophilic form. The most probable factor that governs the permeation of NTXOL base is simply that the MN pores provide a path of least resistance for the poorly skin permeable compound. Thus, the permeation of drug in solution is relatively rapid as compared to NTXOL base through GP skin which received no MN treatment. Secondly, however, solubility of NTXOL base becomes the rate limiting factor as its solubility is very low (≈2.69 mM) as shown by a similar formulation *in vitro*[31]. Very low solubility would ultimately limit solubilized permeation of drug through MN pores. Finally, the *in vivo* pharmacokinetic studies further confirmed the viability of MN created channels during transdermal delivery as did the TEWL readings and microscopic evaluation. Figure 2 shows increases in MN-enhanced plasma levels are most consistent up to 48 h and begin to vary up to 72 h, followed by immediate decreases in levels post patch removal. The pharmacokinetic results for the MN NTXOL base treatment correlate directly with TEWL and visual observation of pores, in that between 48 and 72 h the pores are closing and more variation in plasma levels is observed. The ability of the microneedle to enhance transdermal delivery is clearly evident and it appears that enhanced systemic delivery can be observed for up to 48 h.

If one predicts that the required human therapeutic flux of NTXOL is similar to or less than naltrexone, this target value would be about 34 nmol/cm^2/hr from a 20 cm^2 patch based on the

naltrexone depot injection clinical trial for alcohol dependence. [32] Given a guinea pig NTXOL clearance value of 10 L/h [25] and the MN NTXOL HCl Css of 21 ng/mL, the predicted flux in this animal treatment group is 6 nmol/h through 200 MN pores. Therefore, further optimization of formulation and MN treatment would need to be done in order to treat alcoholism in humans. However, for minimum therapeutic plasma levels for opiate blockade in humans, a naltrexone HCl gel with 4 patches and 400 MN insertions was successful.[33]

Transepidermal water loss

Microneedles can be used as a pretreatment to make skin permeable for subsequent transdermal delivery from a patch or topical formulation. To assess the lifetime of increased skin permeability and therefore the duration of transdermal delivery, we used TEWL to measure skin integrity over time after microneedle treatment. TEWL is an accepted method used in many studies, especially in the cosmetic and dermatology fields, as a measure of skin barrier intensity[34]. TEWL measurements were made every 24 h on occluded skin either treated with microneedles or left untreated (negative control). As shown in Fig. 3(A), occlusion of the skin increased TEWL due to the increased skin hydration caused by occlusion, but treatment with microneedles caused an increased TEWL at 24 and 48 h ($p < 0.05$), but not at 72 h ($p > 0.05$). This indicates that microneedles increased skin permeability for 48 h after treatment when the skin was maintained under occlusion. When a MN array is used on the skin, the rate of water loss from the GP is greater and resulted in higher accumulation of water and a higher TEWL reading. As shown in Fig. 3(B), the skin rapidly recovers in animals (n=6) treated with MN arrays if the animals are left in a non-occlusive (no patch over treated area) environment. Rapid recovery in response to disruption of the stratum corneum by MN application is important to the safety of MN-aided delivery. If failure occurred during the treatment process and microneedle application was not followed by drug placement, rapid healing and normalization of the skin would be expected when left untreated (unoccluded). Overall, TEWL readings proved to be a useful tool in revealing lifetime of the pores created by MN array application in hairless guinea pigs.

Microscopic evaluation of MN created aqueous channels

Similar to TEWL experiments, visual quantification of channel lifetime by microscopic evaluation was employed after MN insertion. The results of microscopic visualization of MN-created pores correlated directly to TEWL findings described earlier. Figure 4 shows the time course of MN treated skin from time zero to 72 h. As shown, there is no staining apparent in the control area of skin. In contrast, as time progresses, the staining is more evident in the 10 min, 24 h, 48 h pictures, and even a slight appearance of staining in the GP skin at 72 h. The observation of apparent staining up to 48 h corresponds directly to significantly elevated TEWL readings. Likewise, at 72 h there was still elevated but not statistically significant water loss in treated areas as there was slight staining of skin, suggesting that by 72 h there is a significant decrease in pore viability and the healing of skin is mostly complete. Based on microscopic evaluation and TEWL readings, MN applications followed by occlusive coverings should be studied for 48-72 h in order to correctly observe permeation through MN-created aqueous channels. These initial studies demonstrate that a single MN pretreatment enables enhanced transdermal delivery from a patch for 48 h and, after removing the occlusion, permits rapid resealing of the skin.

Skin irritation of formulations in hairless guinea pig

An important concern when using gel formulations to study permeation is whether the gel will alter the stratum corneum or cause irritation to the animal, when in intimate contact with the skin. Gels formulated as described in the Methods section proved to cause very little irritation. A similar study that did not involve microneedles but used NTXOL base also showed little or

no irritation to the skin.[35] As can been seen in Fig. 5(A), the “a” value parameter describing skin irritation initially increases but after 24 h, the “a” values are very similar to control, and at 48 h the values are indistinguishable statistically ($p>0.05$). Conversely, an initial decrease in the “L” value was observed, Fig. 5(B), indicating mild erythema but correspondingly, there was rapid reversion to the baseline values. At 48 h post patch removal, there was no observable irritation and no significant difference ($p>0.05$) was observed among “L“ values between NTXOL·HCl, and placebo gel with MN and placebo gel with no MN. Thus, a MN gel patch system is a safe screening method to determine the efficacy of MN and drug combination therapy, resulting in mild to no irritation from the transdermal system.

Conclusions

The ability of the microneedle to bypass the stratum corneum and enhance delivery of water soluble compounds is evident. NTXOL·HCl and NTXOL base as conventional transdermal candidates are poor due to their physicochemical properties, resulting in low plasma concentrations. Even in the presence of MN's, NTXOL base enhancement was low. Conversely, steady state concentration enhancement of NTXOL·HCl after microneedle application was considerably higher than untreated skin or MN treated skin dosed with NTXOL base. Thus, as a transdermal candidate it is the molecule with high aqueous solubility that is successful with MN facilitated delivery. Accordingly, it was shown that MN-created channels were viable for at least 48 h by TEWL, microscopic, and pharmacokinetic evaluation. Irritation from MN treatment followed by NTXOL·HCl showed no significant difference in irritation values from a placebo gel with no MN 48 h post patch removal. These results confirmed that the hairless guinea pig is an appropriate and efficient model for simultaneous evaluation of MN systems, transdermal pharmacokinetics, micropore lifetime, and skin irritation. Finally, these findings suggest that MN assisted delivery of NTXOL·HCl could be an alternative therapy for drug and alcohol addiction.

Acknowledgments

We would like to thank Dr. Mark Allen at Georgia Tech for the use of his microfabrication facilities. This research was supported in part by NIH R01DA13425 and R01EB006369. HSG and MRP are members of the Center for Drug Design, Development and Delivery and the Institute for Bioengineering and Bioscience at Georgia Tech. MRP is the Emerson Lewis Faculty Fellow.

References

1. WHO. The world health report 2001- Mental Health: New Understanding, New Hope. World Health Organization; 2001. ed
2. Harwood HJ, Fountain D, Fountain G. Economic cost of alcohol and drug abuse in the United States, 1992: a report. Addiction 1999;94(5):631–635. [PubMed: 10563025]
3. Mark TL, Coffey RM, Vandivort-Warren R, Harwood HJ, King EC. U.S. spending for mental health and substance abuse treatment, 1991-2001. Health Aff (Millwood) 2005;(Suppl Web Exclusives):W5–133. W135–142. [PubMed: 15797947]
4. Alkermes, C. Vivitrol™ (naltrexone for extended-release injectable suspension). 2006. ed
5. PDR. Generics. second. Medical Economics; New Jersey: 1996. p. 1083-1086.p. 488ed
6. Rukstalis MR, Stromberg MF, O'Brien CP, Volpicelli JR. 6-beta-naltrexol reduces alcohol consumption in rats. Alcohol Clin Exp Res 2000;24(10):1593–1596. [PubMed: 11045869]
7. Stromberg MF, Rukstalis MR, Mackler SA, Volpicelli JR, O'Brien CP. A comparison of the effects of 6-beta naltrexol and naltrexone on the consumption of ethanol or sucrose using a limited-access procedure in rats. Pharmacol Biochem Behav 2002;72(1-2):483–490. [PubMed: 11900823]
8. Ferrari A, Bertolotti M, Dell'Utri A, Avico U, Sternieri E. Serum time course of naltrexone and 6 beta-naltrexol levels during long-term treatment in drug addicts. Drug Alcohol Depend 1998;52(3):211–220. [PubMed: 9839147]

9. McCaul ME, Wand GS, Rohde C, Lee SM. Serum 6-beta-naltrexol levels are related to alcohol responses in heavy drinkers. Alcohol Clin Exp Res 2000;24(9):1385–1391. [PubMed: 11003204]
10. Meyer MC, Straughn AB, Lo MW, Schary WL, Whitney CC. Bioequivalence, dose-proportionality, and pharmacokinetics of naltrexone after oral administration. J Clin Psychiatry 1984;45(9 Pt 2):15–19. [PubMed: 6469932]
11. Wall ME, Brine DR, Perez-Reyes M. Metabolism and disposition of naltrexone in man after oral and intravenous administration. Drug Metab Dispos 1981;9(4):369–375. [PubMed: 6114837]
12. Gerstel, MS.; Place, VA. Office USP. Drug delivery device, Alza Corporation. USA: Alza Corporation; 1976. p. 1-13.ed
13. Gardeniers JGE, Luttge JW, Berenschott JW, de Boer MJ, Yeshurun Y, Hefetz M, van't Oever R, van den Berg A. Silicon micromachined hollow microneedles for transdermal liquid transport. J MEMS 2003;6:855–862.
14. Madou, M. Fundamentals of Microfabrication. Boca Raton, FL: CRC; 1997. ed
15. Cormier M, Johnson B, Ameri M, Nyam K, Libiran L, Zhang DD, Daddona P. Transdermal delivery of desmopressin using a coated microneedle array patch system. J Control Release 2004;97(3):503–511. [PubMed: 15212882]
16. Coulman SA, Barrow D, Anstey A, Gateley C, Morrissey A, Wilke N, Allender C, Brain K, Birchall JC. Minimally invasive cutaneous delivery of macromolecules and plasmid DNA via microneedles. Curr Drug Deliv 2006;3(1):65–75. [PubMed: 16472095]
17. Martanto W, Davis SP, Holiday NR, Wang J, Gill HS, Prausnitz MR. Transdermal delivery of insulin using microneedles in vivo. Pharm Res 2004;21(6):947–952. [PubMed: 15212158]
18. McAllister DV, Wang PM, Davis SP, Park JH, Canatella PJ, Allen MG, Prausnitz MR. Microfabricated needles for transdermal delivery of macromolecules and nanoparticles: fabrication methods and transport studies. Proc Natl Acad Sci U S A 2003;100(24):13755–13760. [PubMed: 14623977]
19. Mikszta JA, Alarcon JB, Brittingham JM, Sutter DE, Pettis RJ, Harvey NG. Improved genetic immunization via micromechanical disruption of skin-barrier function and targeted epidermal delivery. Nature medicine 2002;8(4):415–419.
20. Wermeling DP, Banks SL, Hudson DA, Gill HS, Gupta J, Prausnitz MR, Stinchcomb AL. Microneedles permit transdermal delivery of a skin-impermeant medication to humans. Proc Natl Acad Sci U S A 2008;105(6):2058–2063. [PubMed: 18250310]
21. www.zosanopharma.com. ed
22. www.sanofipasteur.com. ed
23. Kaushik S, Hord AH, Denson DD, McAllister DV, Smitra S, Allen MG, Prausnitz MR. Lack of pain associated with microfabricated microneedles. Anesth Analg 2001;92(2):502–504. [PubMed: 11159258]
24. Ferguson JC, Martin CJ, Rayner C. Burn wound evaporation--measurement of body fluid loss by probe evaporimeter and weight change. Clin Phys Physiol Meas 1991;12(2):143–155. [PubMed: 1855360]
25. Paudel KS, Nalluri BN, Hammell DC, Valiveti S, Kiptoo P, Hamad MO, Crooks PA, Stinchcomb AL. Transdermal delivery of naltrexone and its active metabolite 6-beta-naltrexol in human skin in vitro and guinea pigs in vivo. J Pharm Sci 2005;94(9):1965–1975. [PubMed: 16052561]
26. de Costa BR, Iadarola MJ, Rothman RB, Berman KF, George C, Newman AH, Mahboubi A, Jacobson AE, Rice KC. Probes for narcotic receptor mediated phenomena. 18. Epimeric 6 alpha- and 6 beta-iodo-3,14-dihydroxy-17-(cyclopropylmethyl)-4,5 alpha-epoxymorphinans as potential ligands for opioid receptor single photon emission computed tomography: synthesis, evaluation, and radiochemistry of [125I]-6 beta-iodo-3,14-dihydroxy-17-(cyclopropylmethyl)-4,5 alpha-epoxymorphinan. J Med Chem 1992;35(15):2826–2835. [PubMed: 1322988]
27. Davis SP, Landis BJ, Adams ZH, Allen MG, Prausnitz MR. Insertion of microneedles into skin: measurement and prediction of insertion force and needle fracture force. J Biomech 2004;37(8):1155–1163. [PubMed: 15212920]
28. Gill HS, Prausnitz MR. Coated microneedles for transdermal delivery. J Control Release 2007;117(2):227–237. [PubMed: 17169459]

29. Sutinen R, Paronen P, Saano V, Urtti A. Water-activated, pH-controlled patch in transdermal administration of timolol II. Drug absorption and skin irritation. European Journal of Pharmaceutical Sciences 2000;11:25–31. [PubMed: 10913750]

30. Pierard GE, Pierard-Franchimont C. Dihydroxyacetone test as a substitute for the dansyl chloride test. Dermatology 1993;186(2):133–137. [PubMed: 8428042]

31. Banks SL, Pinninti RR, Gill HS, Crooks PA, Prausnitz MR, Stinchcomb AL. Flux across of microneedle-treated skin is increased by increasing charge of naltrexone and naltrexol in vitro. Pharmaceutical Research 2008;25(7):1677–1685. [PubMed: 18449628]

32. Garbutt JC, Kranzler HR, O'Malley SS, Gastfriend DR, Pettinati HM, Silverman BL, Loewy JW, Ehrich EW. Efficacy and tolerability of long-acting injectable naltrexone for alcohol dependence: a randomized controlled trial. Jama 2005;293(13):1617–1625. [PubMed: 15811981]

33. Wermeling DP, Banks SL, Hudson DA, Gill HS, Gupta J, Prausnitz MR, Stinchcomb AL. Microneedles permit transdermal delivery of a skin-impermeant medication to humans. Proc Natl Acad Sci U S A. 2008

34. Kalia YN, Nonato LB, Guy RH. The effect of iontophoresis on skin barrier integrity: non-invasive evaluation by impedance spectroscopy and transepidermal water loss. Pharm Res 1996;13(6):957–960. [PubMed: 8792440]

35. Paudel, KS.; Hammell, DC.; Gajjella, H.; Stinchcomb, AL. Abstract M1306. Vol. 8. San Antonio, Texas: American Association of Pharmaceutical Sciences; 2006. Skin Irritation and Sensitization of Naltrexone and 6-Beta-Naltrexol in Hairless Guinea Pigs American Association of Pharmaceutical Sciences, Annual Meeting. ed

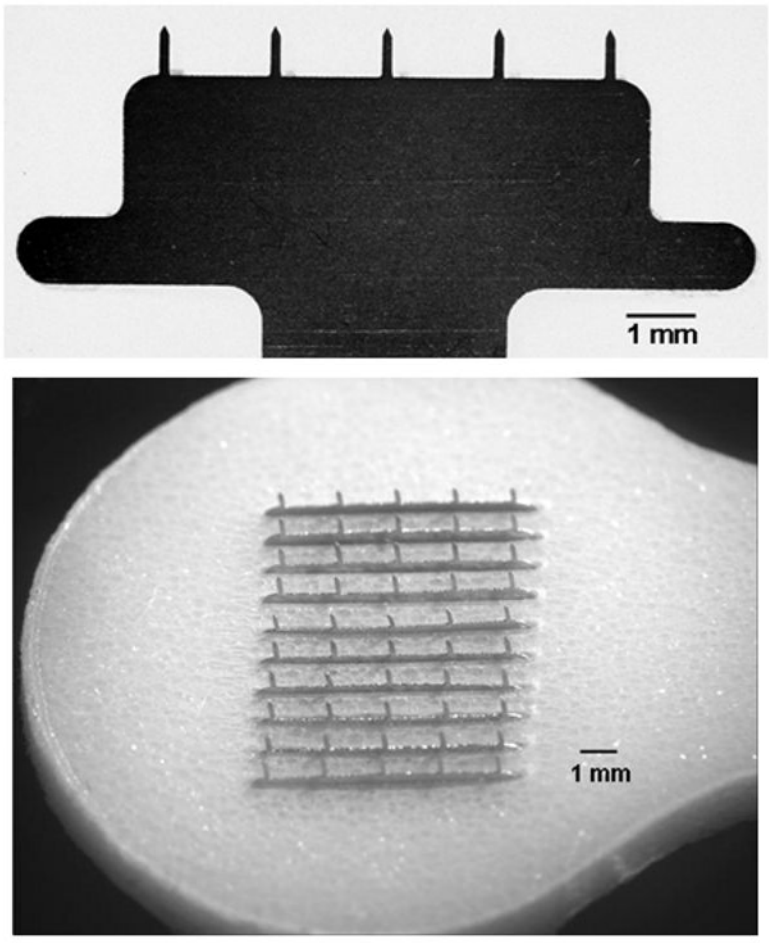

Fig. 1.
In-plane microneedles utilized in skin permeation studies. (A) Brightfield micrograph of a row of five microneedles, (B) brightfield micrograph of a 50 MN array created by assembling 10 sections of five microneedles into polystyrene to form the array.

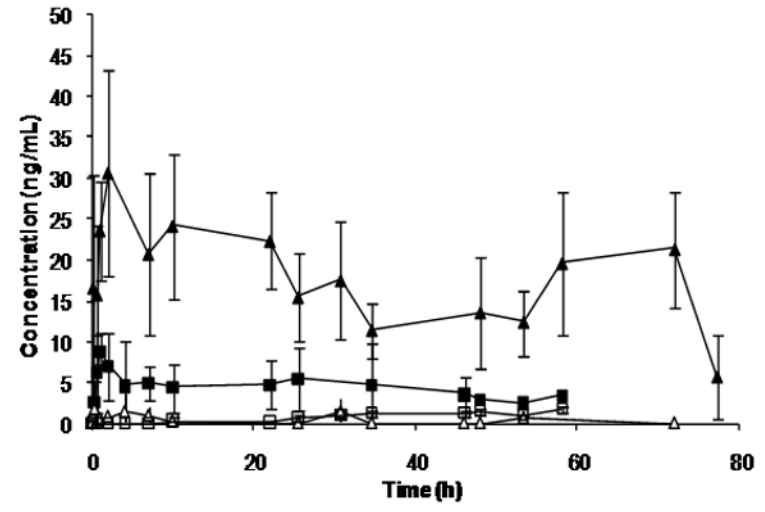

Fig. 2.

In vivo plasma profiles of NTXOL after NTXOL·HCl and NTXOL base with and without microneedle treatment in hairless guinea pigs. GP exposure to gel and patch was 72 h. (-▲- MN NTXOL HCl (n=7), -■- MN NTXOL base (n=3), -Δ- NTXOL HCl no MN (n=3), -□- NTXOL base no MN (n=6))

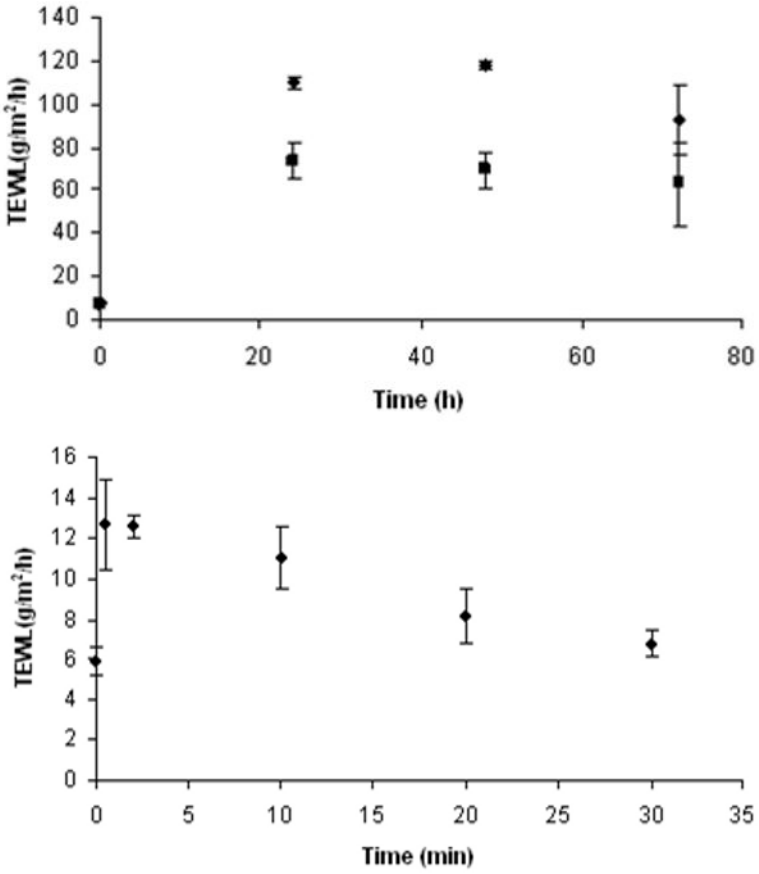

Fig. 3.

In vivo transepidermal water loss studies in hairless guinea pigs. (A) shows the enhanced water loss reading in the presence of microneedles and a significantly lower amount of water loss up to 48 h without microneedle treatment (■-no MN, ◆-MN treated). (B) depicts the rapid recovery of the skin after MN treatment when left unoccluded (◆-MN treated).

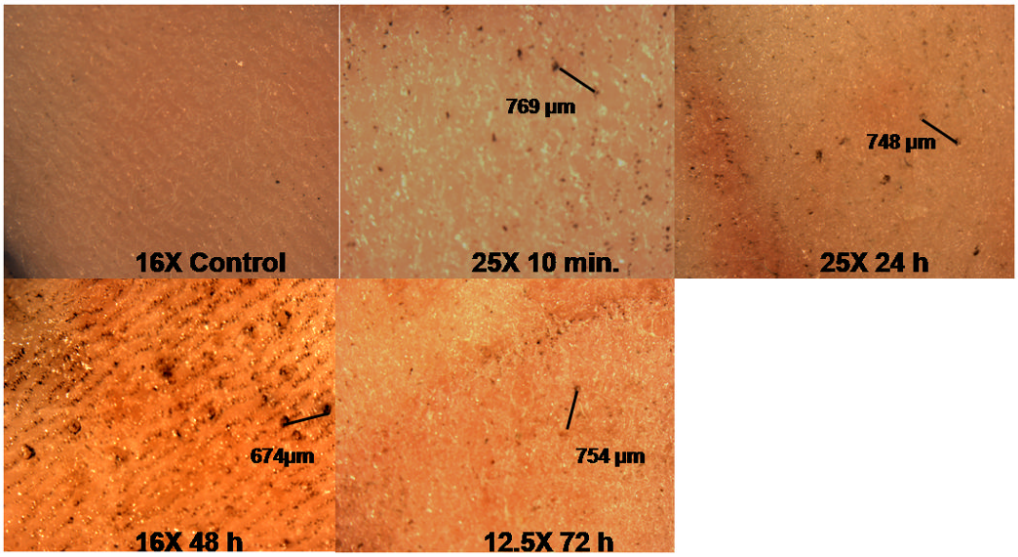

Fig. 4.
Light micrograph of guinea pig skin stained in India ink after *in vivo* microneedle treatment to reveal the presence of MN-created pores over a 72 h time course.

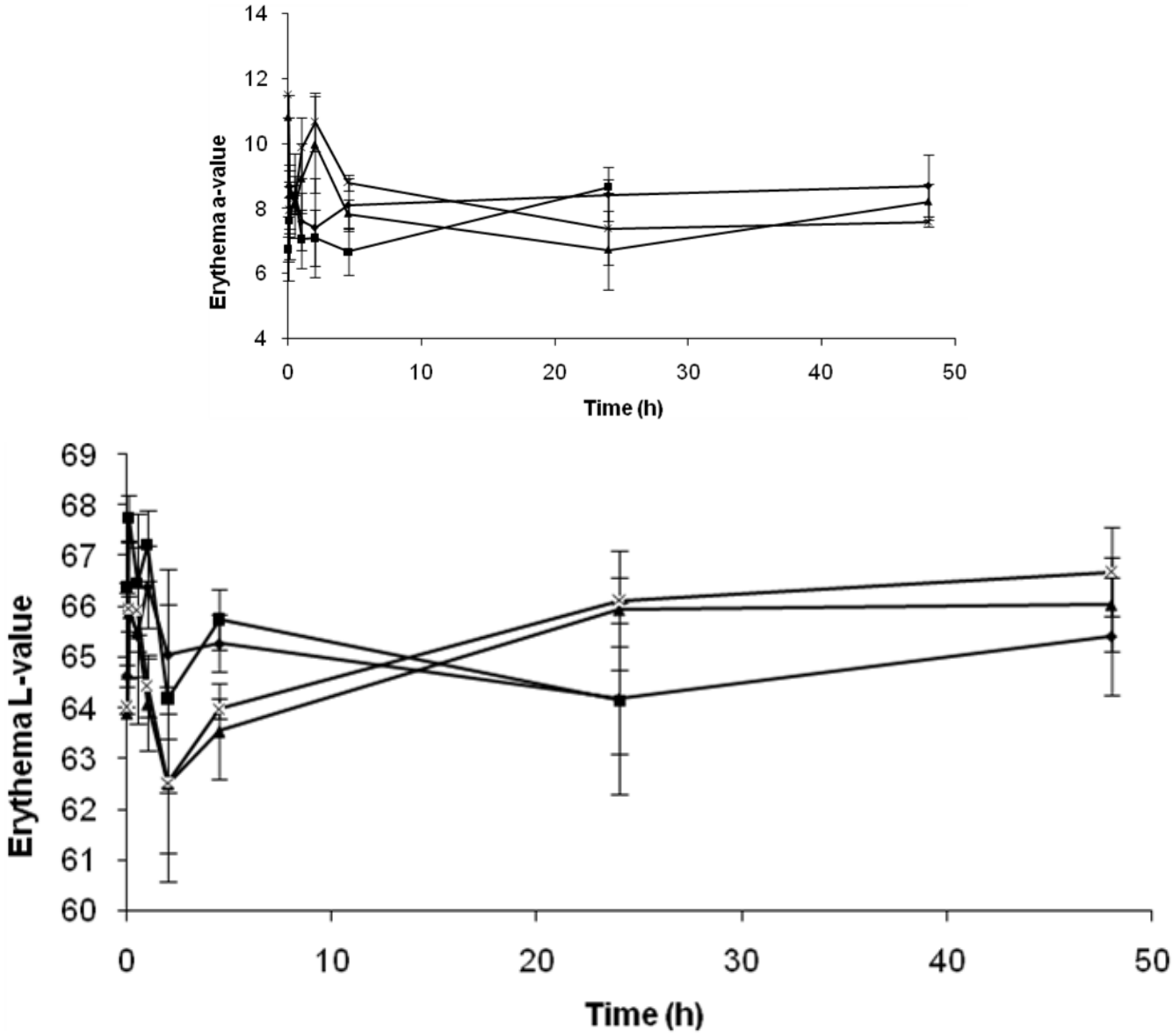

Fig. 5.

In vivo skin irritation of NTXOL base and NTXOL·HCl with MN and placebo gel with and without MN. (A) shows the "a" parameter of skin irritation where an increased value indicates irritation and (B) depicts the "L" parameters where a decrease in value describes erythema. (-◆- MN NTXOL HCl gel, -▲- placebo gel MN, -■- MN NTXOL base, -x- placebo gel no MN)

Table 1

Pharmacokinetic parameters of *in vivo* studies of hairless guinea pigs treated with 26 mg NTXOL base gel, MN application followed by 26 mg NTXOL free base gel, 285 mg NTXOL·HCl gel and MN application followed by 285 mg NTXOL·HCl. The base was saturated in gel whereas the hydrochloride salt remained in a soluble form. The results are reported as mean values ± S.D.

Transdermal Parameters	NTXOL Base	MN NTXOL Base	NTXOL·HCl	MN NTXOL HCl
C_{max} (ng/mL)	1.7 ± 0.5	9.7 ± 1.5	3.3 ± 0.7	48.5 ± 18.8
T_{max} (h)	40.1 ± 11.7	1.0 ± 0.9	12.9 ± 15.7	19.2 ± 11.5
AUC (h*ng/mL)	50.5 ± 10.1	193.2 ± 103.4	18.6 ± 10.0	1349.1 ± 616.7
T_{lag} (h)	5.2 ± 1.6	0.8 ± 0.2	1.0 ± 0.9	0.7 ± 0.3
C_{ss} (ng/mL)	1.0 ± 0.4	5.5 ± 1.9	1.0 ± 0.7	21.3 ± 6.9